Available online at www.sciencedirect.com
SCIENCE DIRECT®
International Journal of Heat and Mass Transfer 47 (2004) 4339–4348
International Journal of HEAT and MASS TRANSFER
www.elsevier.com/locate/ijhmt

Stochastic modeling of evaporating droplets polydispered in turbulent flows

Z. Gao, F. Mashayek *

Department of Mechanical and Industrial Engineering, University of Illinois at Chicago, 842 West Taylor Street, Chicago, IL 60607, USA

Received 10 March 2004; received in revised form 22 April 2004

Abstract

Dispersion and polydispersity of evaporating droplets in turbulent flows are investigated through a newly proposed stochastic model. The model is based on a first-order time series analysis, addresses the anisotropy of turbulence, and adequately takes into account the temporal correlations. It predicts temperature and vapor mass fraction fluctuations as well as velocity fluctuations. A set of averaged equations are derived for the carrier phase in homogeneous turbulence while the interaction between the carrier phase and the droplet phase are considered through source terms. The performance of the model is assessed by conducting simulations of droplet-laden homogeneous shear flows. Good agreements are observed for various velocity, temperature and vapor mass fraction statistics with the DNS data.

1. Introduction

Turbulent flows laden with droplets and particles have been extensively investigated for several decades. There are two categories of approaches to two-phase turbulence modeling. One is the Eulerian–Lagrangian approach, in which the carrier phase is solved in the Eulerian framework and the dispersed phase is solved in the Lagrangian framework. The other is the Eulerian–Eulerian approach, in which both dispersed phase and carrier phase are treated as continuum. Since tracking particles in a Lagrangian framework is more natural, the Eulerian–Lagrangian approach has found wider applications. In this framework, the statistical properties of turbulence are usually determined by solving the Reynolds-averaged Navier–Stokes (RANS) equations. The fluctuations are generated based on the statistical properties, e.g. mean and variance of the fluid fluctuation velocity, by using stochastic tools. The literature [1–7] is rich with previous contributions on development and application of various stochastic models. However, most of the previous works are concentrated on the isothermal turbulence where temperature and vapor mass fraction fluctuations are not considered.

Droplet evaporation can be found in many practical applications, such as liquid fuel combustors, spray drying and chemical power plants. Understandably, more challenges are involved in modeling when the droplets are evaporating and heat and mass transfer is involved. Berlemont et al. [8] studied the heat and mass transfer coupling between vaporizing droplets and turbulence using a Lagrangian approach. Tolpadi et al. [9] proposed a spray model for the prediction of gas turbine combustors. Several other investigations on evaporating sprays in turbulent flows can be found in the literature [10–13]. All of these studies have ignored temperature and vapor mass fraction fluctuations. Moissette et al. [14] proposed a stochastic model to consider the temperature fluctuation in a non-isothermal turbulence, but no evaporation and, therefore, no vapor mass fraction fluctuation was considered.

Recently, we presented a stochastic model [15] for the prediction of velocity and temperature fluctuations in non-isothermal turbulent flows laden with solid particles. The model accounted for anisotropy of turbulence

* Corresponding author. Tel.: +1-312-996-1154; fax: +1-312-413-0047.
E-mail address: mashayek@uic.edu (F. Mashayek).

0017-9310/$ - see front matter © 2004 Elsevier Ltd. All rights reserved.
doi:10.1016/j.ijheatmasstransfer.2004.04.020

Nomenclature

$\vec{A}$	(u, v, w, θ, y) vector of carrier-phase fluctuations
B	transfer number
C_l	droplet specific heat
C_p	fluid specific heat
$\vec{d}$	random vector
d_p	droplet diameter
E_I	normalized internal energy
E_T	normalized total energy
k	carrier-phase turbulence kinetic energy
Le	Lewis number
L_v	latent heat of evaporation
m_p	droplet mass
M_r	$U_\mathrm{r}/\sqrt{\gamma RT_\mathrm{r}}$ reference Mach number
Nu	Nusselt number
P	pressure of the fluid
Pr	$C_\mathrm{p}\mu/\kappa$ Prandtl number
R	gas constant
$R_{\alpha\beta}$	correlation function
S	$d < U_1 > /dx_2$ mean velocity gradient
Sc	Schmidt number
Sh	Sherwood number
S_ϕ	source term, $\phi = m, u_i, e$
t	time
T	temperature
T_L, $T_{\alpha\beta}$	Lagrangian integral time scale
U_i	(U_1, U_2, U_3) instantaneous velocity
u_p	fluctuating velocity of the droplet phase in x_1 direction
v_p	fluctuating velocity of the droplet phase in x_2 direction
w_p	fluctuating velocity of the droplet phase in x_3 direction
x_i	Eulerian spatial coordinates, $i = 1, 2, 3$
X_i	droplet position, $i = 1, 2, 3$
Y	instantaneous vapor mass fraction in the carrier phase
y_s	fluctuating vapor mass fraction at the droplet surface
Y_s	instantaneous vapor mass fraction at the droplet surface

Greek symbols

ϵ	viscous dissipation rate
γ	ratio of the specific heats of the carrier phase
Γ	mass diffusion coefficient
κ	thermal conductivity
μ	dynamic viscosity
ρ	density
θ	fluctuating temperature
τ_p	droplet time constant

Subscripts

p	droplet properties
r	reference parameters
s	properties at the droplet surface
t	time

Superscripts

$'$	Reynolds fluctuating quantity
$''$	Favre fluctuating quantity
$\tilde{}$	Favre averaged quantity
$\vec{}$	vector
T	transpose of a matrix

Other symbol

$\langle\ \rangle$	Reynolds average

and included the effects of the temporal variation of turbulence correlations. In the present paper, we will extend our model to predict the evaporating droplet behavior in compressible turbulence. In Section 2, we discuss the governing equations for the dispersed phase and present the new stochastic model. In Section 3, model performance is assessed by comparison with DNS data. Concluding remarks are provided in Section 4.

2. Dispersed phase equations and modeling

The role of the stochastic model is to provide fluctuating quantities for the fluid at the location of the droplet. These fluctuations are then used along with the mean values, which are calculated separately, to integrate the droplet Lagrangian equations and update its position, X_i, velocity, $U_{p,i}$, temperature, T_p, and mass, m_p. These Lagrangian equations are described, in non-dimensional form, as [16]

$$\frac{\mathrm{d}X_i}{\mathrm{d}t} = U_{p,i}, \tag{1}$$

$$\frac{\mathrm{d}U_{p,i}}{\mathrm{d}t} = \frac{f_1}{\tau_\mathrm{p}}(U_i - U_{p,i}) + g_i, \tag{2}$$

$$\frac{\mathrm{d}T_\mathrm{p}}{\mathrm{d}t} = \frac{f_2}{\tau_\mathrm{p}}(T - T_\mathrm{p}) - \frac{f_3}{\tau_\mathrm{p}}(Y_\mathrm{s} - Y), \tag{3}$$

$$\frac{\mathrm{d}m_\mathrm{p}}{\mathrm{d}t} = -f_4\tau_\mathrm{p}^{1/2}(Y_\mathrm{s} - Y), \tag{4}$$

where U_i, T and Y show the instantaneous fluid velocity, fluid temperature and vapor mass fraction, respectively, at the location of the droplet, and Y_s is the vapor mass fraction at the surface of the droplet.

Since the density ratio of the droplet and the carrier gas is typically large, only the Stokes drag force, with a correction for high droplet Reynolds number, and the gravitational force are retained in the droplet momentum equation. Also, the droplets are assumed to remain spherical and their internal motions are neglected. All the variables are normalized with reference scales for length (L_r), velocity (U_r), temperature (T_r) and density (ρ_r). The non-dimensional droplet time constant, based on the Stokesian drag of a sphere, is

$$\tau_p = \frac{Re_r \rho_p d_p^2}{18}, \tag{5}$$

where d_p and ρ_p are the droplet diameter and density, respectively, and $Re_r = \rho_r U_r L_r/\mu$ with μ denoting the fluid viscosity. The function $f_1 = (1 + 0.15Re_p^{0.687})/(1 + B)$ in (2) represents an empirical correction to the Stokes drag due to large droplet Reynolds numbers and is valid for $Re_p = Re_r \rho d_p |U_i - U_{p,i}| \leqslant 1000$, where $B = (T - T_p)/\lambda$ is the transfer number with $\lambda = L_v/C_P T_r$, and L_v, C_p and ρ representing the latent heat of evaporation, the fluid specific heat at constant pressure and the fluid density, respectively.

The droplets are assumed "lumped" so there is no temperature variation within each droplet. The first term on the right-hand side of (3) represents the rate of change of the droplet temperature due to convective heat transfer with the carrier phase. The factor $f_2 = Nu/3Pr\sigma$ represents a correlation for the convective heat transfer coefficient based on an empirically corrected Nusselt number, $Nu = (2 + 0.6Re_p^{0.5}Pr^{0.33})/(1 + B)$, where $\sigma = C_l/C_p$ with C_l denoting the droplet specific heat, and $Pr = C_p\mu/\kappa$ is the Prandtl number with κ denoting the fluid heat conductivity coefficient. The second term on the right-hand side of (3) represents the change in the droplet internal energy due to phase change. The correlation $f_3 = \rho Sh\lambda/3Sc\sigma$ is a function of an empirically corrected Sherwood number, $Sh = (2 + 0.6Re_p^{0.5}Sc^{0.33})$, where $Sc = \mu/\rho\Gamma$ is the Schmidt number with Γ denoting the binary mass diffusivity coefficient.

The vapor mass fraction at the surface of the droplet is equal to the vaporization pressure (P_{vap}) of the droplet (for equivalent molecular weights of the gas and the liquid) and obeys the Clausius–Clapeyron equation

$$Y_s = P_{vap} = \frac{P_B}{P} \exp\left[\frac{\gamma\lambda}{(\gamma - 1)T_B}\left(1 - \frac{T_B}{T_p}\right)\right], \tag{6}$$

where the boiling temperature, T_B, and pressure, P_B, of the liquid are assumed to be constant. Finally, (4) governs the rate of mass transfer from the droplet due to evaporation which is a function of the vapor mass fraction difference at the droplet surface, the droplet time constant, and the Sherwood-number-dependent correlation

$$f_4 = \pi\left(\frac{18}{\rho_p}\right)^{0.5} \frac{\rho Sh}{Re_r^{1.5}Sc}. \tag{7}$$

2.1. Stochastic model

The stochastic model needed to obtain the fluctuations is a generalization of the model presented in our previous work [15], where a general framework was formed for simulation of temperature and velocity fluctuations. The model is based on the method of time series analysis [17] and is extended here to simulate the species fluctuations. We use the notation u, v, w, θ and y to denote fluctuations in the fluid velocity (in x_1, x_2 and x_3 directions), temperature and vapor mass fraction, respectively, at the droplet location. These fluctuating quantities at time t can be expressed as a linear aggregate of previous values at time $t - \delta t$ and a white noise which is independent of the process,

$$\vec{A}_t = \boldsymbol{\beta} \cdot \vec{A}_{t-\delta t} + \vec{d}_t, \tag{8}$$

where boldface shows a tensor, and

$$\vec{A}_t = \begin{pmatrix} u_t \\ v_t \\ w_t \\ \theta_t \\ y_t \end{pmatrix},$$

$$\boldsymbol{\beta} = \begin{pmatrix} \beta_{uu} & \beta_{uv} & \beta_{uw} & \beta_{u\theta} & \beta_{uy} \\ \beta_{vu} & \beta_{vv} & \beta_{vw} & \beta_{v\theta} & \beta_{vy} \\ \beta_{wu} & \beta_{wv} & \beta_{ww} & \beta_{w\theta} & \beta_{wy} \\ \beta_{\theta u} & \beta_{\theta v} & \beta_{\theta w} & \beta_{\theta\theta} & \beta_{\theta y} \\ \beta_{yu} & \beta_{yv} & \beta_{yw} & \beta_{y\theta} & \beta_{yy} \end{pmatrix}, \tag{9}$$

$$\vec{d}_t = \begin{pmatrix} d_{tu} \\ d_{tv} \\ d_{tw} \\ d_{t\theta} \\ d_{ty} \end{pmatrix}.$$

Here $\vec{d}_t$ is a white noise vector with zero mean and independent of $\vec{A}_t$.

To solve for the fluctuations, the expressions for $\boldsymbol{\beta}$ and $\vec{d}_t$ need to be determined. The method used for derivation of these expressions is similar to that explained in our previous papers [15,18]; here we only present the final results. The expression for $\boldsymbol{\beta}$ reads

$$\boldsymbol{\beta} = \boldsymbol{C} \cdot \mathbf{cov}^{(-1)}(\vec{A}_{t-\delta t}, \vec{A}_{t-\delta t}^T), \tag{10}$$

where

$$\boldsymbol{C}(\delta t)=\begin{pmatrix} R_{uu}\sqrt{\overline{u_t^2}}\sqrt{\overline{u_{t-\delta t}^2}} & R_{uv}\sqrt{\overline{u_t^2}}\sqrt{\overline{v_{t-\delta t}^2}} & \cdots & R_{uy}\sqrt{\overline{u_t^2}}\sqrt{\overline{y_{t-\delta t}^2}} \\ R_{vu}\sqrt{\overline{v_t^2}}\sqrt{\overline{u_{t-\delta t}^2}} & R_{vv}\sqrt{\overline{v_t^2}}\sqrt{\overline{v_{t-\delta t}^2}} & \cdots & R_{vy}\sqrt{\overline{v_t^2}}\sqrt{\overline{y_{t-\delta t}^2}} \\ \vdots & \vdots & \vdots & \vdots \\ R_{yu}\sqrt{\overline{y_t^2}}\sqrt{\overline{u_{t-\delta t}^2}} & R_{yv}\sqrt{\overline{y_t^2}}\sqrt{\overline{v_{t-\delta t}^2}} & \cdots & R_{yy}\sqrt{\overline{y_t^2}}\sqrt{\overline{y_{t-\delta t}^2}} \end{pmatrix} \tag{11}$$

and $R_{\alpha\beta}(\delta t)$ is the correlation function assumed in the following exponential form:

$$R_{\alpha\beta}(\delta t)=\frac{\overline{\alpha\beta}}{\sqrt{\overline{\alpha^2}}\sqrt{\overline{\beta^2}}}\exp\left(\frac{\delta t}{T_{\alpha\beta}}\right), \tag{12}$$

where α and β represent u, v, w, θ or y.

The solution for $\vec{d}_t$ reads

$$\vec{d}_t=\boldsymbol{B}\cdot\vec{Z}, \tag{13}$$

where $\boldsymbol{B}$ is a matrix, and can be determined by using Cholesky factorization of matrix $\mathbf{cov}(\vec{d}_t,\vec{d}_t^{\mathrm{T}})$ according to the following relation:

$$\boldsymbol{B}\cdot\boldsymbol{B}^{\mathrm{T}}=\mathbf{cov}(\vec{d}_t,\vec{d}_t^{\mathrm{T}}), \tag{14}$$

and $\vec{Z}$ is a random vector, each component of which is independently sampled from a standard normal distribution with a mean of zero and a variance of unity.

To conduct the simulations, the Lagrangian integral time scales $T_{\alpha\beta}$ must be known in advance. The adequate description of various turbulence scales remains as one of the most important problems in particle tracking process as also discussed by Berlemont et al. [19], and the determination of the Lagrangian integral time scale is one of the most critical steps for the development of the stochastic particle dispersion models. A popular form for expressing the time scale is

$$T_{\mathrm{L}}=C_{\mathrm{T}}\frac{k}{\epsilon}, \tag{15}$$

where C_{T} is a constant varying between 0.135 and 0.56, and k and ϵ denote the fluid turbulence kinetic energy and its rate of dissipation, respectively.

Due to the lack of information on various time scales, in our simulations we assume $T_{\alpha\beta}=T_{\mathrm{L}}$ for all velocity correlations. It has been shown that particle dispersion is sensitive to the value of the constant C_{T}, and different values have been assigned in different flow simulations in conjunction with various models [8]. (The interested reader is referred to the literature [1,20–23] for further discussion.) Recently, Simonin et al. [24] suggested a constant value of 0.482 for incompressible turbulent shear flow simulation, which was later adopted by Zaichik [25]. However, no previous research has been found on the time scale in compressible homogeneous shear flow; therefore, some tests have to be conducted first. The existing information on time scales for temperature and mass fraction correlations is even more scarce. Several different time scales are tested here, and the predicted results are assessed by comparison with DNS data.

3. Model assessment

The flow considered here is a compressible homogeneous shear turbulence for which DNS data are available for comparison from the study of Mashayek [16] for a homogeneous shear flow, where the carrier phase and the dispersed phase are solved in Eulerian and Lagrangian frames, respectively. For comparison purposes, we consider in this study the same set of equations as that used in the DNS study. The droplet Lagrangian equations are presented in Section 2. Below we describe the Eulerian equations for the carrier phase in both instantaneous and averaged forms.

3.1. Carrier-phase governing equations

The carrier phase (composed of the gas and the vapor) is considered to be a compressible, Newtonian fluid with zero bulk viscosity, and to obey the perfect gas equation of state. The instantaneous density, velocity, pressure and temperature of the carrier phase are denoted by ρ, U_i, P and T, respectively. The instantaneous vapor mass fraction is denoted by Y. The evaporating droplets interact with the carrier phase, and the two-way coupling effects must be taken into account for an accurate representation of the flow. Here, we introduce source terms $\mathscr{S}_{\mathrm{m}}$, $\mathscr{S}_{\mathrm{ui}}$ and $\mathscr{S}_{\mathrm{e}}$ to consider the two-way coupling effects for mass, momentum and energy, respectively. With this nomenclature, the Eulerian forms of the non-dimensional continuity, momentum, and energy equations for the carrier phase are given by

$$\frac{\partial\rho}{\partial t}+\frac{\partial}{\partial x_j}(\rho U_j)=\mathscr{S}_{\mathrm{m}}, \tag{16}$$

$$\frac{\partial}{\partial t}(\rho U_i)+\frac{\partial}{\partial x_j}(\rho U_iU_j)=-\frac{\partial P}{\partial x_i}+\frac{2}{Re_{\mathrm{r}}}\frac{\partial}{\partial x_j}\left(S_{ij}-\frac{1}{3}\Delta\delta_{ij}\right)+\mathscr{S}_{\mathrm{ui}}, \tag{17}$$

$$\frac{\partial E_T}{\partial t}+\frac{\partial}{\partial x_j}[U_j(E_T+P)] = \frac{1}{(\gamma-1)Re_r Pr M_r^2}\frac{\partial^2 T}{\partial x_j \partial x_j}+\frac{2}{Re_r}\frac{\partial}{\partial x_j}\left[U_i\left(S_{ij}-\frac{1}{3}\Delta\delta_{ij}\right)\right]+\mathscr{S}_e, \tag{18}$$

and the conservation equation for the vapor mass fraction is described as

$$\frac{\partial}{\partial t}(\rho Y)+\frac{\partial}{\partial x_j}(\rho Y U_j)=\frac{1}{Re_r Sc}\frac{\partial^2 Y}{\partial x_j \partial x_j}+\mathscr{S}_m, \tag{19}$$

along with the equation of state $P=\rho T/\gamma M_r^2$, where $M_r=U_r/\sqrt{\gamma R T_r}$ is the reference Mach number with R denoting the gas constant. All the fluid variables are normalized with the same reference scales used for the droplet variables.

The total energy (E_T) is the summation of the sensible internal energy ($\rho C_v T$, where C_v is the specific heat of the carrier phase) and the kinetic energy ($\frac{1}{2}\rho U_i U_i$) of the gas–vapor mixture. In the above equations, $\Delta = U_{j,j}$ is the dilatation ($U_{i,j}=\partial U_i/\partial x_j$), $S_{ij}=\frac{1}{2}(U_{i,j}+U_{j,i})$ is the rate-of-strain tensor, and δ_{ij} is the Kroenecker delta function. The specific enthalpies for the gas and the liquid are described as $h_g = T$ and $h_l = \sigma T$, respectively. In DNS, only the case with $\sigma = 1$ is considered, for which the specific enthalpy of the vapor is expressed as $h_v = T + \lambda$. All the enthalpies are normalized by $C_p T_r$. The total energy Eq. (18) is derived by assuming unity Lewis number ($Le \equiv Sc/Pr = 1$).

The source/sink terms $\mathscr{S}_m$, $\mathscr{S}_{ui}$, and $\mathscr{S}_e$ appearing in (16)–(18) represent the integrated effects of the droplets mass, momentum, and energy exchange with the carrier phase. These Eulerian variables are calculated from the Lagrangian droplet variables by volume averaging the contributions from all of the individual droplets residing within the cell volume ($\delta\mathscr{V}=(\delta x)^3$, where δx is the node spacing) centered around each grid point. These terms are expressed as

$$\mathscr{S}_m = -\frac{1}{\delta\mathscr{V}}\sum^{n_p}\frac{dm_p}{dt}, \tag{20}$$

$$\mathscr{S}_{ui} = -\frac{1}{\delta\mathscr{V}}\sum^{n_p}\left[\frac{d}{dt}(m_p U_{p,i})\right], \tag{21}$$

$$\mathscr{S}_e = -\frac{1}{\delta\mathscr{V}}\sum^{n_p}\left[\frac{1}{(\gamma-1)M_r^2}\frac{d}{dt}(m_p T_p) - \frac{\lambda}{(\gamma-1)M_r^2}\frac{dm_p}{dt}+\frac{d}{dt}\left(\frac{1}{2}m_p U_{p,i}^2\right)\right], \tag{22}$$

where n_p is the number of droplets within the cell volume and those cells with $n_p = 0$ are assigned a zero value for each variable.

3.2. Carrier-phase averaged equations

In this section, we derive transport equations for carrier-phase averaged variables. When implemented in conjunction with the stochastic model for fluctuating variables, these averaged equations provide a complete framework for simulation of droplet-laden, compressible homogeneous shear flow.

For a general instantaneous variable f, the following decompositions are applied:

$$f = \langle f\rangle + f' = \tilde{f} + f'', \tag{23}$$

where $'$ and $''$ denote fluctuating quantities, $\langle\ \rangle$ refers to Reynolds average quantity and $\tilde{}$ refers to Favre averaged quantity. For homogeneous shear flow, it is shown that these two averages are equivalent [26]. Furthermore, recognizing that

$$\frac{\partial\langle f\rangle}{\partial x_i}=0 \tag{24}$$

for all the variables, except the mean streamwise velocity, the averaged equations can be simplified significantly for homogeneous shear flow. After some algebraic manipulations [27], the final averaged equations are described as

$$\frac{\partial\langle\rho\rangle}{\partial t}=\langle S_m\rangle \tag{25}$$

for the carrier-phase density, and

$$\frac{\partial\langle Y\rangle}{\partial t}=\frac{1}{\langle\rho\rangle}(1-\langle Y\rangle)\langle S_m\rangle \tag{26}$$

for the vapor mass fraction. Since the mean carrier-phase velocity in homogeneous shear flow is known as $\langle U_i\rangle = S x_2 \delta_{i1}$, where $S = d\langle U_1\rangle/dx_2 = \text{constant}$, we do not need the momentum equation.

To obtain an equation for the mean temperature, we write the internal energy E_I as [16]

$$E_I=\frac{\rho(T/\gamma+Y\lambda)}{(\gamma-1)M_r^2}, \tag{27}$$

which upon averaging yields

$$\langle E_I\rangle=\frac{1}{(\gamma-1)M_r^2}\left[\frac{1}{\gamma}(\langle\rho\rangle\langle T\rangle+\langle\rho' T'\rangle)+\lambda(\langle\rho\rangle\langle Y\rangle+\langle\rho' Y'\rangle)\right]. \tag{28}$$

The analysis of the DNS data shows that correlations $\langle\rho' Y'\rangle$ and $\langle\rho' T'\rangle$ can be neglected. As a result, rearranging (28) yields the following equation for the mean temperature:

$$\langle T\rangle=\frac{\gamma}{\langle\rho\rangle}\left[(\gamma-1)M_r^2\langle E_I\rangle-\lambda\langle\rho\rangle\langle Y\rangle\right]. \tag{29}$$

To proceed, the average source term $\langle \mathscr{S}_m \rangle$ is expressed as

$$\langle \mathscr{S}_m \rangle = -\frac{1}{(2\pi)^3} \sum^{n_p} \frac{d\langle m_p \rangle}{dt}, \tag{30}$$

where n_p is the total number of droplets in the simulation box which has a volume of $(2\pi)^3$ in DNS. Finally, the transport equation for $\langle E_I \rangle$ in homogeneous flow is given as [16]

$$\frac{\partial \langle E_I \rangle}{\partial t} = \epsilon + \frac{S^2}{Re_r} - \frac{1}{(\gamma-1)M_r^2(2\pi)^3} \sum^{n_p} \left(m_p \frac{dT_p}{dt} + T_p \frac{dm_p}{dt} \right). \tag{31}$$

3.3. Results and discussion

The stochastic simulations are conducted following exactly the same initial conditions as in the DNS. Our numerical methodology for stochastic simulation is the same as in our previous papers [15,18] and is not repeated here for brevity. The carrier phase fluctuating quantities are directly imported from DNS results into stochastic simulations and comparisons are presented here for various carrier-phase mean variables and droplet mean and fluctuating variables.

We first concentrate on the validation of the mean flow variables. Fig. 1 shows temporal variation of various mean variables and comparisons with the DNS data. The time axis in the figure is normalized by the inverse of the shear rate S. The droplets are released into the flow at $St = 0$, but they start evaporating at $St = 2$. This is evident from Fig. 1 which clearly shows different behaviors before and after $St = 2$. Before the evaporation of the droplets begins, the fluid internal energy E_I includes only the gas part and is increasing slightly due mainly to the energy added to the system by the mean velocity gradient. After the evaporation begins, the carrier phase includes both the gas and the vapor, and the internal energy exhibits a sudden increase due to the addition of the vapor internal energy. It should be noted that the simulations are conducted for a periodic box without any net exchange of mass, momentum or energy with the surroundings. As a result, the density of the carrier phase increases in time because of the mass transfer from the droplets to the gas by evaporation.

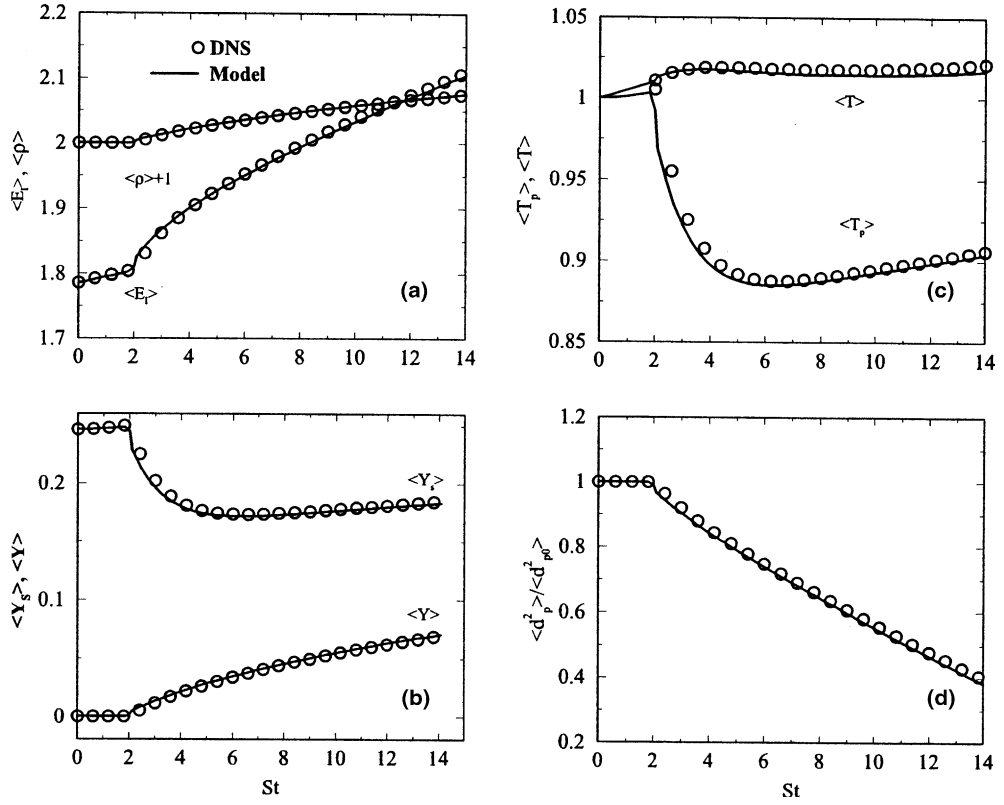

Fig. 1. Mean properties comparison between simulation and DNS data: (a) internal energy and density of the carrier phase; (b) vapor mass fraction of the carrier phase and its magnitude at the droplet surface; (c) temperatures of the carrier phase and the droplets; (d) droplet diameter squared.

(Note that the curve for the mean density has been shifted upward as $\langle\rho\rangle + 1$ so that it can be shown on the same graph with the internal energy.)

The temporal variation of the vapor mass fraction at the surface of the droplet, $\langle Y_s\rangle$, is of great importance in predicting the droplet evaporation. It is observed in Fig. 1(b) that the mean vapor mass fraction at the surface of the droplet sharply decreases immediately after the evaporation begins. This is because the initial difference of the mass fraction at the surface of the droplet and that in the carrier phase is large. After some time, the evaporation process approaches an equilibrium with the heat transfer process, and the mass fraction begins to increase due to the heat transfer from the gas. The temporal evolution of the vapor mass fraction in the carrier phase, $\langle Y\rangle$, is also shown in Fig. 1(b). The mean mass fraction is increasing continuously after the evaporation starts, because evaporation always contributes to the increase of the amount of vapor in the carrier phase. It is also noted that, in the absence of chemical reaction, there is no mechanism for consumption of vapor in the simulation. Fig. 1(c) shows the temporal variations of the carrier phase and the droplets mean temperatures. The droplet temperature exhibits a sharp

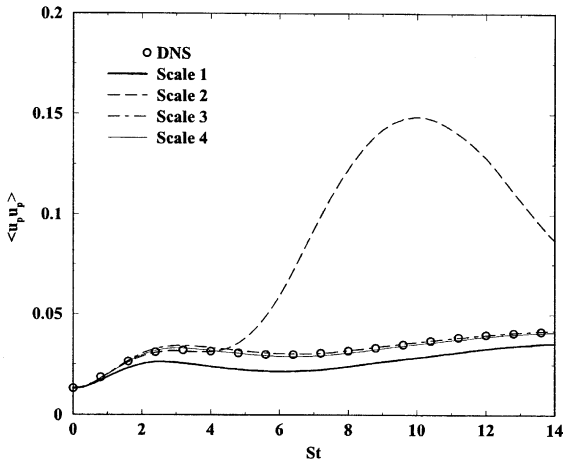

Fig. 2. The effect of time scale on droplet velocity fluctuation in the streamwise direction (Scale 1, $T_L = 0.482\frac{k}{\epsilon}$; Scale 2, $T_L = 1.98$; Scale 3, $T_L = 2 \times 0.482\frac{k}{\epsilon}$; Scale 4, $T_L = 1.8 \times 0.482\frac{k}{\epsilon}$).

decrease immediately after the evaporation begins, which is a very similar behavior to that of the vapor mass fraction at the surface of the droplet. This is because during the initial stages of evaporation the energy

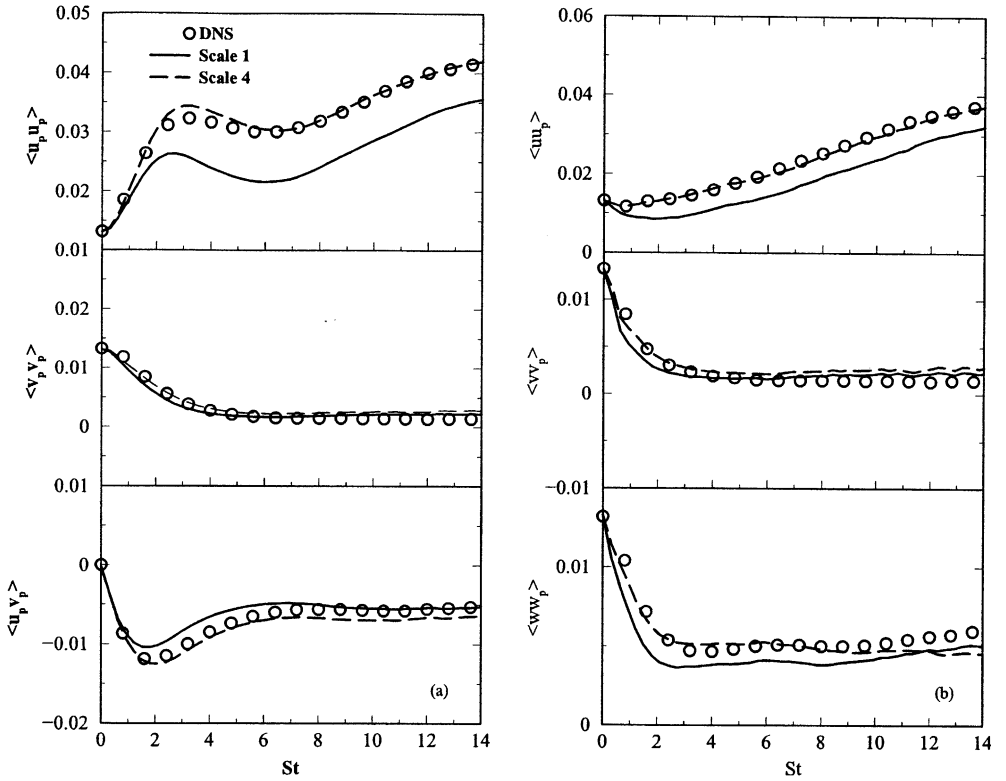

Fig. 3. Temporal evolution of droplet velocity correlations and fluid-droplet velocity cross-correlations (Scale 1, $C_T = 0.482$; Scale 4, $C_T = 1.8 \times 0.482$).

needed for phase change is provided by the decrease of the droplet internal energy.

To study the evaporation rate, the temporal variation of the mean-squared droplet diameter $\langle d_p^2\rangle/d_{p0}^2$ is plotted in Fig. 1(d), where d_{p0} is the initial droplet diameter. It is noted that, the rate of change of the mean-squared droplet diameter is linear after a short initial stage. This behavior is in agreement with the classical d^2-law [28,29]. The deviation from the linear trend at the initial stage can be explained by considering the temporal variations of the mean vapor mass fraction at the surface of the droplet and the droplet temperature as discussed above. All the results in Fig. 1 suggest that the modeled average equations are perfectly capable of reproducing the DNS results.

Next, we focus our attention on fluctuating variables. To accurately predict the droplet statistics, a time scale must be determined first for the velocity correlation. Fig. 2 shows the results for $\langle u_p u_p\rangle$ velocity correlations calculated based on four time scales, where u_p is the droplet fluctuating velocity in the streamwise direction. Scale 1 is the time scale from Eq. (15), and Scale 2 is a constant value of 1.98 obtained by regressing the DNS data of $\langle u(t)u(t-\delta t)\rangle$ for $St < 4$. Scale 3 is two times Scale 1, and Scale 4 is 1.8 times Scale 1. From Fig. 2, it is observed that Scale 1 yields smaller values for $\langle u_p u_p\rangle$; however, it captures the trend of variation quite closely to the DNS data. Scale 2 gives good results for $St < 4$, but afterwards its predictions deviate significantly from the DNS data. This is because the regression is based on the data for $St < 4$, and there are no provisions for adjusting the time scale as k and ϵ change in time. Scale 3 provides very good comparison with the DNS data during the entire simulation. Scale 4 is slightly smaller than Scale 3, and the simulation results are accordingly improved. As a result, Scale 4 is the choice for time scale for this turbulent flow. The main reason for introducing the coefficient 1.8 is that the DNS is for a much lower Reynolds number as compared to laboratory flows based on which Eq. (15) is proposed. The following results are based on this time scale; however, for comparison we also present the results based on Scale 1.

All the statistics of the dispersed phase and the fluid-droplet cross-correlations are obtained through our stochastic model; here only some of the results are presented. Fig. 3(a) shows the temporal evolution of the droplet normal stresses in streamwise and cross-stream directions as well as the shear stress of the droplets. Fig. 3(b) shows the time evolution of the fluid-droplet velocity cross-correlations in all three directions. In this figure, we have used v_p and w_p to denote the droplets fluctuating velocities in cross-stream and spanwise directions, respectively. It is clear that the simulation results are in good agreement with the DNS data, and the model can properly predict various velocity correlations of the evaporating droplets in this turbulent flow.

To address the temperature and mass fraction fluctuation correlations, the choice of time scale again is a very important issue. As compared to velocity correlation, temperature and mass fraction fluctuation correlations have much less information available from the existing literature; therefore, it is more difficult to assign an appropriate form. We start by regressing the DNS data to an exponential function, and then make some adjustments based on the comparison of the simulation results with the DNS data. Fig. 4(a) shows the root mean square (rms) value of the vapor mass fraction fluctuation at the droplet surface. A variety of time scales have been tested; only three are discussed here. Scale 1 is taken as a uniform value, $T_Y = 0.1$. For Scale 2, we assume the time scale for mass fraction correlation is proportional to that for velocity correlation, so the expression for T_Y becomes $T_Y = C_Y C_T \frac{k}{\epsilon}$, with $C_Y = 0.1$ and $C_T = 0.482$. Scale 3 takes stepwise values in time, which varies from 0.1 to 0.28, somewhat in a curve-fitting manner. As witnessed from the figure, neither the uniform time scale nor the scale proportional to that for

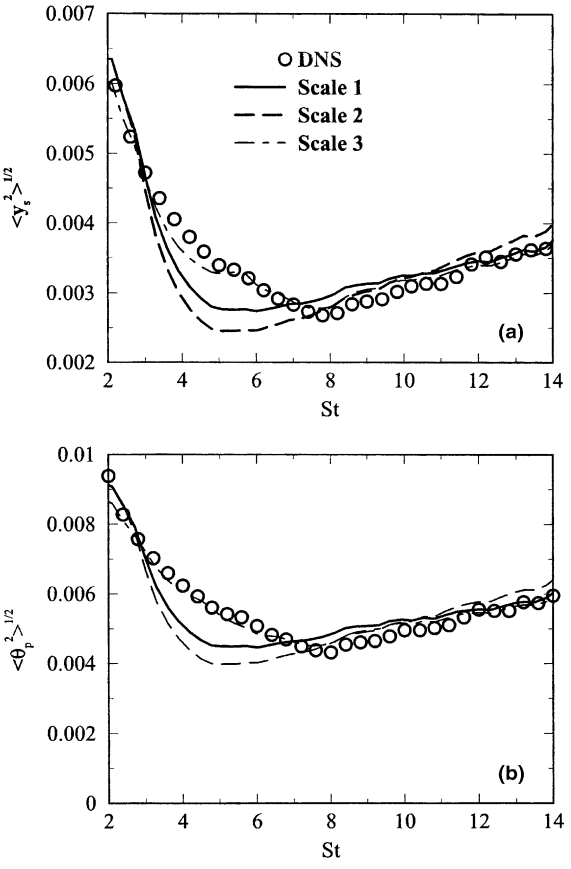

Fig. 4. Temporal evolution of the root mean square of (a) vapor mass fraction fluctuation at droplet surface and (b) droplet temperature fluctuation (Scale 1, uniform $T_Y = 0.1$; Scale 2, $C_Y C_T \frac{k}{\epsilon}$; Scale 3, non-uniform $T_Y = 0.1$–0.28).

velocity correlation are capable of providing a good comparison for $3 < St < 7$. However, the stepwise non-uniform scale can be adjusted to yield a very good agreement with the DNS data for the entire simulation. Following the same idea, we simulated the rms of the droplet temperature fluctuation, and the results are presented in Fig. 4(b). Similarly, three different time scales are presented here and, again, the stepwise non-uniform time scale yields the best comparison with the DNS data.

4. Conclusions

The droplet evaporation in a low-Mach number homogeneous shear flow is investigated using a new stochastic model for predicting the vapor mass fraction fluctuations as well as the droplet velocity and temperature fluctuations. The proposed stochastic model is developed using the method of time-series analysis, and accounts for temporal correlations and anisotropy of the turbulence. The cross-correlations among various components of the velocity, temperature and vapor mass fraction are also taken into account. Appropriate Lagrangian integral time scales for velocity, temperature and mass fraction are discussed. The mean flow field of the carrier phase is calculated by solving the averaged governing equations. Various statistics, including the droplet turbulence correlations and the fluid-droplet turbulence cross-correlations are obtained through the stochastic model. Comparison with the available DNS data, shows good agreements for various statistics. Nevertheless, the results are sensitive to the choice of the time scale, in agreement with previous observations reported in the literature. The proper description of the time scale for temperature and passive scalar remains as a very important subject in turbulence research in the future.

Acknowledgements

The support for this work was provided by the US Office of Naval Research under grant N00014-01-1-0122 with Dr. G.D. Roy as Program Officer and from the National Science Foundation under grant CTS-0237951 with Dr. T.J. Mountziaris as Program Director.

References

[1] A.D. Gosman, E. Ioannides, Aspects of computer simulation of liquid-fuelled combustors, AIAA Paper 81-0323, 1981.
[2] A. Ormancey, J. Martinon, Prediction of particle dispersion in turbulent flows, PhysicoChem. Hydrodynam. 5 (3) (1984) 229–244.
[3] E. Etasse, C. Meneveau, T. Poinsot, Simple stochastic model for particle dispersion including inertia, trajectory-crossing, and continuity effects, ASME J. Fluid Eng. 120 (1998) 186–192.
[4] Y. Wang, P.W. James, On the effect of anisotropy on the turbulent dispersion and deposition of small particles, Int. J. Multiphase Flow 25 (3) (1999) 551–558.
[5] Q.Q. Lu, An approach to modeling particle motion in turbulent flows—I. Homogeneous, isotropic turbulence, Atmos. Environ. 29 (3) (1995) 423–436.
[6] F. Mashayek, Stochastic simulations of particle-laden isotropic turbulent flow, Int. J. Multiphase Flow 25 (8) (1999) 1575–1599.
[7] P. Pascal, B. Oesterle, On the dispersion of discrete particles moving in a turbulent shear flow, Int. J. Multiphase Flow 26 (2) (2000) 293–325.
[8] A. Berlemont, M.-S. Grancher, G. Gouesbet, On the Lagrangian simulation of turbulence influence on droplet evaporation, Int. J. Heat Mass Transfer 34 (11) (1991) 2805–2812.
[9] A.K. Tolpadi, S.K. Aggarwal, H. Mongia, An advanced spray model for application to the prediction of gas turbine combustor flowfields, Numer. Heat Transfer A 38 (4) (2000) 325–340.
[10] A.S.P. Solomon, J.-S. Shuen, Q.-F. Zhang, G.M. Faeth, A theoretical and experimental study of turbulent evaporating sprays, NASA CR 174760, 1984.
[11] G.M. Faeth, Evaporation and combustion in sprays, Prog. Energy Combust. Sci. 19 (1983) 1–76.
[12] G.M. Faeth, Mixing, transport and combustion in sprays, Prog. Energy Combust. Sci. 13 (1987) 293–345.
[13] A.J. Shearer, H. Tamura, G.M. Faeth, Evaluation of locally homogeneous flow model of spray evaporation, J. Energy 3 (5) (1979) 271–278.
[14] S. Moissette, B. Oesterle, P. Boulet, Temperature fluctuations of discrete particles in a homogeneous turbulent flow: a Lagrangian model, Int. J. Heat Fluid Flow 22 (3) (2001) 220–226.
[15] Z. Gao, F. Mashayek, Stochastic model for non-isothermal droplet-laden turbulent flows, AIAA J. 42 (2) (2004) 255–260.
[16] F. Mashayek, Droplet-turbulence interactions in low-Mach-number homogeneous shear two-phase flows, J. Fluid Mech. 367 (1998) 163–203.
[17] G.E.P. Box, G.M. Jenkins, Time Series Analysis, Holden-Day, Oakland, CA, 1976.
[18] Z. Gao, F. Mashayek, A stochastic model for gravity effects in particle-laden turbulent flows, J. Fluids Eng., in press.
[19] A. Berlemont, P. Desjonqueres, G. Gouesbet, Particle tracking in turbulent flows, in: Proceedings of the ASME Gas–Solid Flows Conference, Washington, DC, 1993, pp. 121–131.
[20] J.-S. Shuen, L.-D. Chen, G.M. Faeth, Evaluation of a stochastic model of particle dispersion in a turbulent round jet, AIChE J. 29 (1983) 167–170.
[21] P. Chen, C. Crowe, On the Monte Carlo method for modeling particle dispersion in turbulence, ASME FED 10 (1984) 37–42.
[22] R.V. Calabrese, S. Middleman, The dispersion of discrete particles in a turbulent fluid field, AIChE J. 25 (1979) 1025–1035.

[23] S. Elghobashi, T. Abou-Arab, M. Rizk, A. Mostafa, Prediction of the particle-laden jet with a two-equation turbulence model, Int. J. Multiphase Flow 10 (6) (1984) 697–710.
[24] O. Simonin, E. Deutsch, M. Boivin, Large eddy simulation and second-moment closure model of particle fluctuating motion in two-phase turbulent shear flows, in: F. Durst, N. Kasagi, B. Launder, F. Schmidt, J. Whitelaw (Eds.), Turbulent Shear Flows 9, Springer-Verlag, 1995, pp. 85–115.
[25] L.I. Zaichik, A statistical model of particle transport and heat transfer in turbulent shear flows, Phys. Fluids 11 (6) (1999) 1521–1534.
[26] G.A. Blaisdell, N.N. Mansour, W.C. Reynolds, Compressibility effects on the growth and structure of homogeneous turbulent shear flow, J. Fluid Mech. 256 (1993) 443–485.
[27] Z. Gao, Stochastic modeling and simulation of particle/droplet-laden turbulent flows, Ph.D. Thesis, University of Illinois at Chicago, Chicago, IL, 2003.
[28] D.B. Spalding, The combustion of liquid fuels, in: Proceedings of the 4th Symposium (International) on Combustion, The Combustion Institute, Baltimore, MD, 1953, pp. 847–864.
[29] G.A.E. Godsave, Studies of the combustion of drops in a fuel spray, in: Proceedings of the 4th Symposium (International) on Combustion, The Combustion Institute, Baltimore, MD, 1953, pp. 818–830.